

A Ruthenium Bridge in Fullerene–Ferrocene Arrays: Synthesis of $[\text{Ru}(\text{C}_{60}\text{Me}_5)\text{R}(\text{CO})_2]$ ($\text{R} = \text{C}_6\text{H}_4\text{Fc}$, $\text{C} \equiv \text{CFc}$) and Their Charge-Transfer Properties

Yutaka Matsuo,^{*,[a]} Keiko Matsuo,^[a] Takeshi Nanao,^[b] Renata Marczak,^[c]
S. Shankara Gayathri,^[c] Dirk M. Guldi,^{*,[c]} and Eiichi Nakamura^{*,[a, b]}

Abstract: New fullerene–ferrocene arrays, $[\text{Ru}(\text{C}_{60}\text{Me}_5)(\text{C}_4\text{H}_6\text{Fc})(\text{CO})_2]$ (Fc = ferrocenyl) and $[\text{Ru}(\text{C}_{60}\text{Me}_5)(\text{CCFc})(\text{CO})_2]$, in which the ruthenium complex functions as a conjugative bridge, were synthesized by the reaction of $[\text{Ru}(\text{C}_{60}\text{Me}_5)\text{Cl}(\text{CO})_2]$ with $\text{FcC}_6\text{H}_4\text{MgBr}$ and FcCCLi , respectively. These compounds were investigated by electrochemical measurement, single-crystal X-ray structural analysis, and

photophysical measurement. Upon photoirradiation, the former compound was converted rapidly into the corresponding triplet state in toluene ($\tau_{\text{singlet}} = 21$ ps), whereas the charge-separated state was predominant in THF

($\tau_{\text{singlet}} = 10.5$ ps; $\tau_{\text{CS}} = 355$ ps). The latter compound, on the other hand, formed the charge-separated state in both toluene and THF ($\tau_{\text{singlet}} = 3.0$ ps; $\tau_{\text{CS}} = 152$ ps). Thus, the structural difference between the phenylene and acetylene bridges in **1** and **2**, respectively, was found to change the outcome of the photophysical processes.

Keywords: allenylidenes • charge transfer • ferrocene • fullerenes • ruthenium

Introduction

Ever since the initial discovery of fullerenes, scientists worldwide have studied the solid-state properties of these molecules, which range from superconductivity to applications in nanostructure devices.^[1] The spherical structure of

fullerenes, which consist exclusively of electron-rich hexagons and electron-deficient pentagons, evoked lively interest in relating their properties to conventional one-dimensional π systems. The extraordinary electron-acceptor properties of, for example, the most abundant fullerene, C_{60} , which has a diameter of 7.8 Å, have led to the ingenious utilization of such nanoscale architectures in light-induced electron-transfer studies and solar-energy conversion.^[2] It is mainly the small reorganization energy, which fullerenes exhibit in electron-transfer reactions, that accounts for the noteworthy developments in these areas.^[3] In particular, ultrafast charge separation together with very slow charge recombination lead to the formation of unprecedented long-lived radical-ion-pair states in high quantum yields.^[4] Ferrocenes are frequently employed as either the terminal electron donor or part of a redox chain in electron-transfer relay systems, owing to their ease of oxidation. The combination of these remarkable electron-accepting and -donating properties, respectively, has resulted in noteworthy advances in photoinduced charge separation and has, thus, attracted interest in the area of solar-energy-conversion systems.^[5]

Metallic bridges have, for instance, been implemented between the donor and acceptor moieties as mediators or initiators for photoinduced charge-separation processes. Metal-

[a] Dr. Y. Matsuo, Dr. K. Matsuo, Prof. Dr. E. Nakamura
Nakamura Functional Carbon Cluster Project, ERATO
Japan Science and Technology Agency
7-3-1 Hongo, Bunkyo-ku
Tokyo, 113-0033 (Japan)
Fax: (+81)3-5841-1476
Fax: (+81)3-5800-6889
E-mail: matsuo@chem.s.u-tokyo.ac.jp
nakamura@chem.s.u-tokyo.ac.jp

[b] T. Nanao, Prof. Dr. E. Nakamura
Department of Chemistry
The University of Tokyo
7-3-1 Hongo, Bunkyo-ku
Tokyo, 113-0033 (Japan)

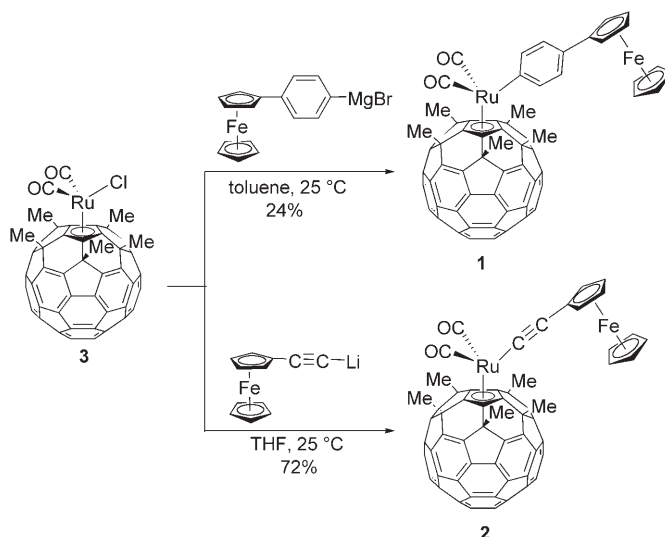
[c] Dr. R. Marczak, Dr. S. S. Gayathri, Prof. Dr. D. M. Guldi
Department of Chemistry and Pharmacy and
Interdisciplinary Center for Molecular Materials
Friedrich-Alexander-Universität
Erlangen-Nürnberg (Germany)
E-mail: dirk.guldi@chemie.uni-erlangen.de

containing groups such as metalloporphyrins are known to act as chromophores, which expedite/promote electron-transfer processes from the ferrocene part to the fullerene part under visible-light irradiation.^[6] Moreover, the use of metalloporphyrins has been beneficial in achieving long-lived radical-ion-pair states.^[7] However, reports of such metal-connected arrays have been rather limited, and the results have been, in general, less clear-cut than desired.^[8] We asked ourselves the question about the photophysical behavior of a compound in which a metal atom is bonded to the fullerene in an η^5 - π manner.^[9,10] Does the metal atom act as a mediator, a suppresser, or cause unexpected behavior? Another motivation for this investigation concerns the wide diversity of η^5 - π -fullerene-metal complexes relative to the numerous organometallic compounds containing fullerene in which the metal and the fullerene moieties are connected but also separated by organic groups, as exemplified by the well-known fulleropyrrolidine unit.^[11] We therefore anticipated that such metal- η^5 -fullerene complexes would allow us to create a new class of donor-metal-acceptor arrays. Herein, we report the synthesis and charge-separation features of new fullerene-ruthenium-ferrocene linked arrays, $[\text{Ru}(\text{C}_{60}\text{Me}_5)\text{R}(\text{CO})_2]$ ($\text{R} = \text{C}_6\text{H}_4\text{Fc}$ and $\text{C}\equiv\text{CFc}$; Fc = ferrocenyl). A detailed photophysical investigation revealed that placing a ruthenium atom directly on the fullerene core accelerates the singlet-to-intersystem crossing, and that the occurrence of the charge-separated state depends on the structure around the metal center.

Results and Discussion

Synthesis and Characterization of $[\text{Ru}(\text{C}_{60}\text{Me}_5)(\text{C}_6\text{H}_4\text{Fc})(\text{CO})_2]$ (**1**) and $[\text{Ru}(\text{C}_{60}\text{Me}_5)(\text{C}\equiv\text{CFc})(\text{CO})_2]$ (**2**)

The synthesis of the dyads **1** and **2** was achieved by the direct coupling of a ruthenium-fullerene complex with a ferrocene-containing magnesium or lithium reagent (Scheme 1). Thus, the treatment of a ruthenium-penta(methyl)[60]fullerene-chloro complex, $[\text{Ru}(\text{C}_{60}\text{Me}_5)\text{Cl}(\text{CO})_2]$ (**3**),^[12] with a ferrocenylphenyl Grignard reagent in THF at 50 °C afforded $[\text{Ru}(\text{C}_{60}\text{Me}_5)(\text{C}_6\text{H}_4\text{Fc})(\text{CO})_2]$ (**1**) as a red powder in 34% yield (Scheme 1a). Compound **1** was stable in air as a solid for over 6 months. A direct bond between the ruthenium atom and the ferrocenyl groups failed to



Scheme 1. Synthesis of the ruthenium η^5 -pentamethyl[60]fullerene complexes bearing the ferrocenyl group.

form without the phenylene bridge, which is probably due to the steric bulk of the fullerene moiety. $[\text{Ru}(\text{C}_{60}\text{Me}_5)(\text{C}\equiv\text{CFc})(\text{CO})_2]$ (**2**) was synthesized by a similar procedure. Reaction of **3** with ferrocenylethynyllithium in THF at 25 °C gave **2** in 72% yield (Scheme 1b). Both compounds were soluble in aromatic solvents, carbon disulfide (CS_2), chloroform, methylene chloride, and THF, and insoluble in acetonitrile, alcohols, and water. These ruthenium-fullerene complexes were purified by preparative HPLC equipped with Cosmosil Buckyprep columns (Nacalai Tesque, Inc.) followed by recrystallization from CS_2 , which gave black crystals of **1** and **2**.

Compounds **1** and **2** were characterized by combustion analysis, atmospheric pressure chemical ionization mass spectrometry (APCI-MS), UV/Vis, IR, and NMR spectroscopy, and X-ray crystallographic analysis. The UV/Vis spectra of **1** and **2** exhibited a spectral pattern characteristic of neutral penta(organo)[60]fullerene derivatives^[13] with absorption maxima at $\lambda = 350$ and 390 nm, which indicates the absence of ground-state intramolecular charge separation. In the ^{13}C NMR spectrum of **2**, signals due to the ethynyl carbon atoms were observed in the typical ethyne region at $\delta = 121.82$ (Ru-C) and 106.42 ppm (Fc-C). The IR spectrum of **2** exhibited asymmetric and symmetric stretching vibrations of the carbonyl groups at 2040 and 1994 cm^{-1} as well as a C=C stretching vibration of the bridge at 2040 cm^{-1} . The CO vibration frequencies are similar to those found for the starting material **3** (2045 and 1999 cm^{-1}), which indicates the absence of the inductive electron-donating effect of the ferrocenylethynyl group in the ground state of **2**. The C=C stretching frequency of **2** is comparable to that of the related pentamethylcyclopentadienyl compound $[\text{Ru}(\text{C}_5\text{Me}_5)(\text{PPh}_3)_2(\text{C}\equiv\text{CFc})]$ ($\nu(\text{C}\equiv\text{C}) = 2072 \text{ cm}^{-1}$).^[14]

Single crystals of **1** and **2** were obtained by the slow diffusion of ethanol into a solution of **1** in carbon disulfide and a solution of **2** in chlorobenzene, respectively. X-ray crystallo-

Abstract in Japanese:

フラーレン-ルテニウム-フェロセン連結分子 $[\text{Ru}(\text{C}_{60}\text{Me}_5)\text{R}(\text{CO})_2]$ ($\text{R} = \text{C}_6\text{H}_4\text{Fc}$ and $\text{C}\equiv\text{CFc}$; Fc = ferrocenyl) を合成し、電気化学測定、X線結晶構造解析を行い、光物性を調べた。THF 中では2種類の分子はともに、照射下において非常に速い電荷分離状態形成を示したが、トルエン中では、フェニレン架橋分子は三重項励起状態へ、アセチレン架橋分子は電荷分離状態へ至ること明らかにした。この特性の違いは、アセチレン架橋分子において励起状態がルテニウムアレーニリデン構造を取り得ることや、アセチレンはフェニレンよりも電子的相互作用を受け渡ししやすいことに由来すると考えられる。

graphic analysis was performed to confirm the molecular structures and to approximate the distances between the fullerene and ferrocene parts (Figures 1 and 2). The average

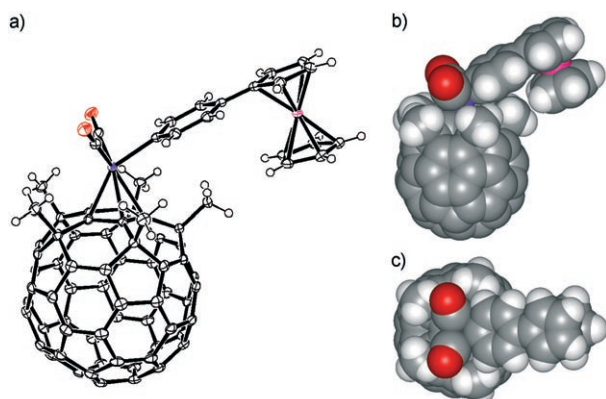


Figure 1. Crystal structure of **1**. a) ORTEP drawing with ellipsoids at the 30% probability level. b) Side view of the space-filling model. c) Top view of the space-filling model.

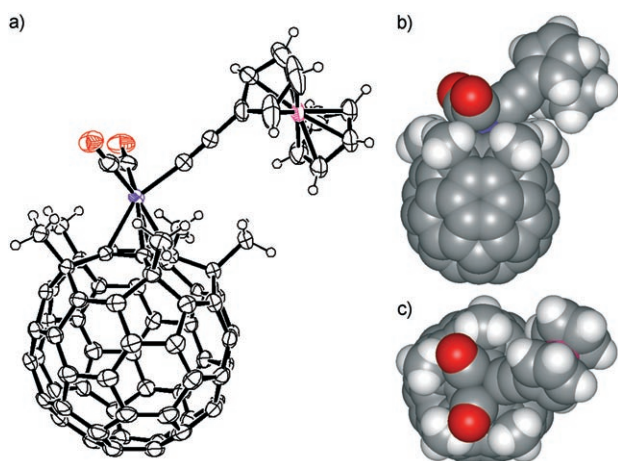


Figure 2. Crystal structure of a single molecule of **2-PhCl**. Solvent molecules are omitted for clarity. a) ORTEP drawing with ellipsoids at the 30% probability level. b) Side view of the space-filling model. c) Top view of the space-filling model.

distance between the center of gravity of C_{60} and the iron atom for **1** and **2** was estimated to be 10.40 and 9.67 Å, respectively, which implies that the donor–acceptor distance is shorter in **2** than in **1**. In the crystal packing of **1**, a pairwise arrangement of the molecules was observed (Figure 3). This molecular arrangement suggests the presence of weak electronic interactions between the fullerene and the ferrocene moiety in the solid state. This interaction may account for the very dark color of these complexes.

Electrochemical Investigations

Cyclic voltammetric measurements were conducted to probe the donor–acceptor properties of **1** and **2** in solution. Compound **1** underwent one reversible one-electron-oxidation

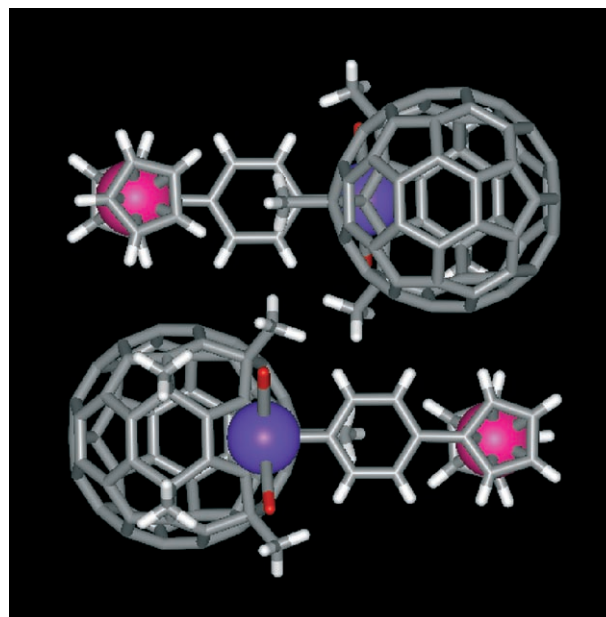


Figure 3. A pair of molecules of compound **1** as found in the crystal.

step of the ferrocene moiety at $E_{1/2} = -0.01$ V and two reversible one-electron-reduction steps of the fullerene moiety at $E_{1/2} = -1.33$ and -1.83 V (Figure 4). The two reduction potentials of **1** are roughly comparable to those reported for $C_{60}Me_5$ and $C_{60}Ph_5$ metal complexes.^[15] Of note is the stability upon one-electron oxidation and one-electron reduction. This stability offered an opportunity to study the photoinduced charge-separation processes. It was reported that metal–fullerene complexes are often reduced irreversibly because of cleavage of the metal–fullerene bonds upon reduction.^[15c]

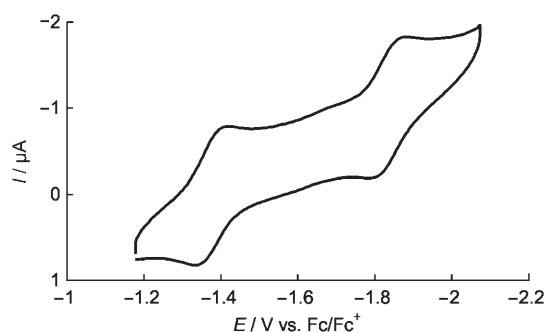


Figure 4. Cyclic voltammogram of **1** in THF containing nBu_4NClO_4 as the supporting electrolyte (scan rate 100 mV s^{-1}) recorded at 25°C .

Compound **2** exhibited a reversible one-electron-oxidation step of the ferrocene moiety at $E_{1/2} = -0.02$ V and a reversible one-electron-reduction step of the fullerene part at $E_{1/2} = -1.35$ V, followed by an irreversible one-electron-reduction step of the fullerene part at $E_p = -1.84$ V. The first reduction potential of **2** is slightly higher than that for $[Ru(C_{60}Me_5)(C\equiv CPh)(CO)_2]$, which has a PhCC group instead

FULL PAPERS

of the FcCC group ($E_{1/2} = -1.32$ V for **1** and -1.91 V for **2**).^[12] We estimated the HOMO–LUMO energy gaps on the basis of the oxidation and reduction potentials of the ferrocene and fullerene moieties ($E_{1/2}^{\text{ox}} - E_{1/2}^{\text{red}}$) to be 1.32 and 1.33 eV for **1** and **2**, respectively. Despite the similar energy gap, the photoinduced charge-separation behavior of the two compounds were found to be quite different from each other.

Photophysical and Intramolecular Charge-Separation Properties

Both donor–acceptor conjugates **1** and **2** were examined by steady-state fluorescence spectroscopy in toluene and THF at room temperature (Table 1). The penta(organo)-

Table 1. Photophysical properties of $C_{60}Me_5H$, $[Fe(C_{60}Me_5)Cp]$, **1**, and **2**.

Compound	Fluorescence quantum yield (ϕ)		τ (singlet) [ps]		τ (radical ion pair) [ps]	
	THF	Toluene	THF	Toluene	THF	Toluene
$C_{60}Me_5H$	2.2×10^{-3}	2.2×10^{-3}	650	705	— ^[a]	— ^[a]
$[Fe(C_{60}Me_5)Cp]$	1.6×10^{-5}	2.4×10^{-5}	0.7	0.8	28	35
1	0.8×10^{-4}	1.0×10^{-4}	10.5	21	355	— ^[a]
2	1.1×10^{-4}	1.2×10^{-4}	3.0	5.5	152	≈ 100

[a] No radical-ion-pair formation was observed.

hydro[60]fullerene $C_{60}Me_5H$,^[13b,16] with a fluorescence maximum at 615 nm and a fluorescence quantum yield of 2.2×10^{-3} (in toluene and THF), was used as a reference system. The donor–acceptor conjugates **1** and **2** exhibited a significant quenching of the fullerene-centered fluorescence relative to that of $C_{60}Me_5H$ (Figure 5). Such quenching is indicative of an accelerated deactivation of the singlet excited state. The fluorescence quantum yields for **1** and **2** were 1.0×10^{-4} and 1.2×10^{-4} in toluene and 0.8×10^{-4} and 1.1×10^{-4} in THF, respectively. These small differences may be ascribed to the variations in the donor–acceptor distances (see above) and/or solvent-polarity dependences.

In the next step, transient absorption measurements were carried out for **1** and **2** in toluene and THF to shed light on the nature of the products evolving from the intramolecular deactivation. Monitoring of the time evolution of the characteristic features of the singlet excited state of C_{60} is a convenient way to identify the spectral features of the resulting photoproducts and to determine the absolute rate constants for the intramolecular decay.

We first investigated the transient absorption spectra of the fullerene reference, $C_{60}Me_5H$. As the corresponding time–absorption profiles indicate, the singlet excited states were formed nearly instantaneously, which is likely to involve internal deactivation starting from the energetically higher-lying excited states. Typical features of the singlet–singlet transitions are maxima in the visible range at 580 nm and at 900 nm in the near-infrared (NIR) region.^[17] Multiwavelength analysis of the singlet decay reveals singlet-excited-state lifetimes of (705 ± 10) ps. These lifetimes imply an effi-

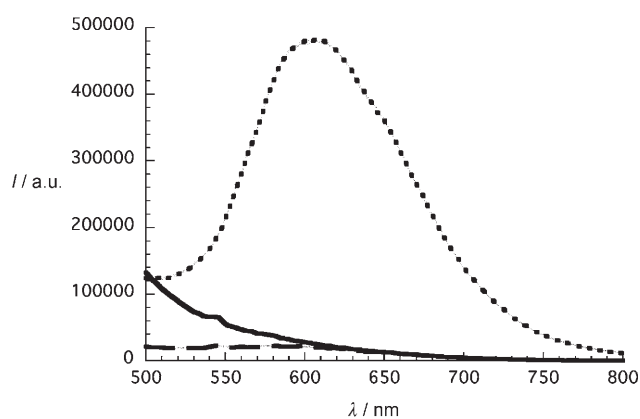


Figure 5. Room-temperature fluorescence spectra of $C_{60}Me_5H$ (dotted line), **1** (dashed line), and **2** (solid line) in toluene recorded with solutions that exhibit an optical absorption of 0.14 (a.u.) at an excitation wavelength of 400 nm.

cient spin-forbidden intersystem crossing that transforms the singlet excited states into the energetically lower-lying triplet excited states. The transient absorption spectra of the corresponding triplet excited states show maxima at 665 nm. This was confirmed independently by recording the spectra at the end of the femtosecond experiment timescale and at the beginning of the nanosecond experiment timescale.

Next, we examined the donor–acceptor complex **1**. Of particular importance is the observation of the fullerene singlet excited state in all the experiments. This observation attests to the successful photoexcitation of the fullerene core. Regardless of the solvent polarity and donor–acceptor composition, the fullerene singlet excited state decayed with accelerated dynamics, relative to the reference system. In **1**, the fullerene singlet excited state decayed with lifetimes of 21 and 10.5 ps in toluene and THF, respectively. Such a solvent-dependent acceleration suggests, at first glance (kinetic analysis), the presence of intramolecular charge-separation processes. However, upon closer inspection of the spectroscopic changes, two different photoproducts were identified. Figure 6 reveals that in toluene the spectroscopic marker of the fullerene triplet excited state, namely, a maximum at 655 nm, evolved simultaneously with the decay of the singlet excited state (maxima at 580 and 900 nm). This led us to conclude that a heavy-atom effect by the ruthenium atom is responsible for the rapid intersystem crossing. Notably, the similarly bound ruthenocene $[Ru(C_{60}Me_5)Cp]$ (Cp = cyclopentadienyl)^[18] was shown to lead to the same reactivity, albeit with somewhat weaker impact (190 ps).^[10] On the contrary, the spectral features in THF bear no resemblance with those of the fullerene triplet excited state; the transient maximum at 655 nm was not observed in THF. Instead, we see in Figure 7 that a series of absorption bands with maxima at 450, 555, 1025, and 1295 nm grew with kinetics that are practically identical to that of the singlet decay. The NIR fingerprint bears close resemblance to those seen for a variety of fullerenes and fullerene derivatives.^[19] In the visible region, on the other hand, the transient spectrum match-

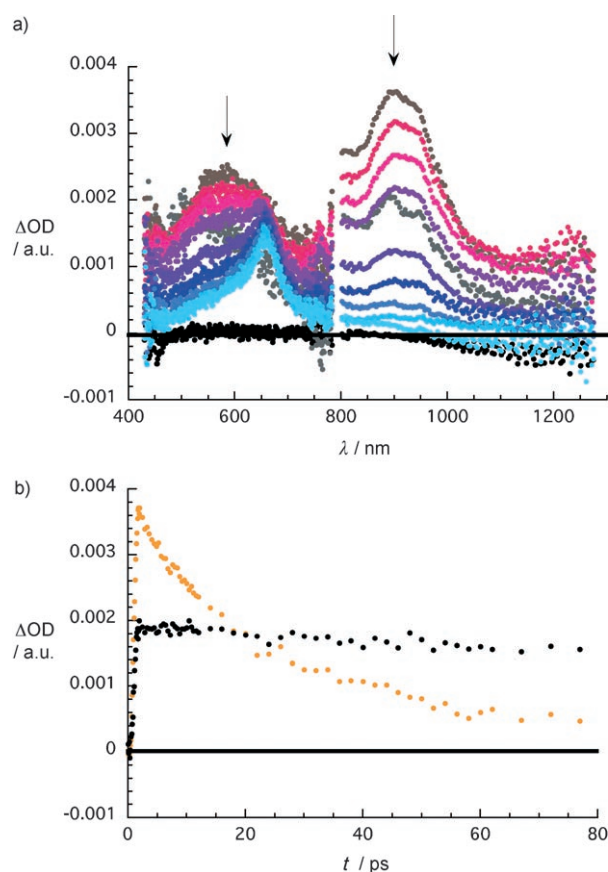


Figure 6. a) Differential absorption spectra (visible and NIR) obtained upon femtosecond flash photolysis (387 nm, 150 nJ) of **1** in nitrogen-saturated toluene with several time delays between 0 and 100 ps at room temperature. OD is the optical density. The arrows indicate the temporal evolution. b) Time-absorption profiles of the spectra shown above at 655 (black) and 900 nm (orange), monitoring the singlet-to-triplet intersystem crossing.

es completely that of the charge-separated state generated in a series of buckyferrocenes.^[10] It is safe to assume that the driving force for the charge separation in toluene is insufficient to compete with the accelerated intersystem crossings (heavy-atom effect). This is apparently different in THF, in which the charge separation occurs twice as fast. The radical-ion-pair state is, however, metastable and decays on the timescale of several hundred picoseconds back to the ground state. For THF as a solvent, we determined a decay lifetime of 355 ps.

An alternative strategy of accelerating the charge separation suggests better electronic coupling between the donor and acceptor moieties. The reduction of the spatial separation, for example, is a probate approach. In fact, this is realized in the ferrocenylethynyl derivative **2**. Both THF and toluene support intramolecular charge separation, as evidenced by the spectroscopic markers of the fullerene radical anion^[20] throughout the visible (450 and 555 nm) and NIR region (1020 and 1195 nm) (Figure 8). In the context of the dynamics of accelerated intersystem crossings, which apparently dominate the photophysics of the aforementioned

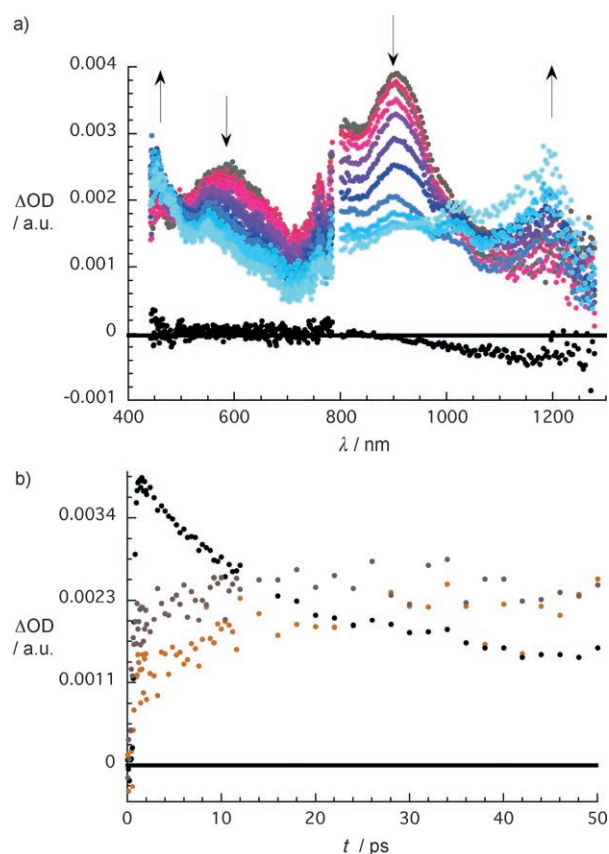


Figure 7. a) Differential absorption spectra (visible and NIR) obtained upon femtosecond flash photolysis (387 nm, 150 nJ) of **1** in nitrogen-saturated THF with several time delays between 0 and 100 ps at room temperature. The arrows indicate the temporal evolution. b) Time-absorption profiles of the spectra shown above at 450 (brown), 900 (black), and 1200 nm (red), monitoring the charge separation.

compound **1**, no spectroscopic evidence that would imply involvement of the formation of a fullerene triplet excited state was obtained for **2**. Interestingly, both processes (charge separation and charge recombination) were notably accelerated. In particular, lifetimes of 3.0 ps for charge separation and 152 ps for charge recombination, which were measured in THF, reflect the closer spacing of the donor and acceptor moieties.^[21]

Conclusions

We have synthesized new fullerene–ferrocene dyads **1** and **2** by the coupling of a fullerene core with a ferrocene unit through a Ru metal atom and a conjugative bridge, and demonstrated, through photophysical measurements, the competition between photoinduced charge separation and accelerated intersystem crossing (heavy-atom effect). The outcome of the photophysical processes depends on the bridging motifs. Upon photoirradiation, compound **1** converts rapidly into the corresponding triplet state in toluene,

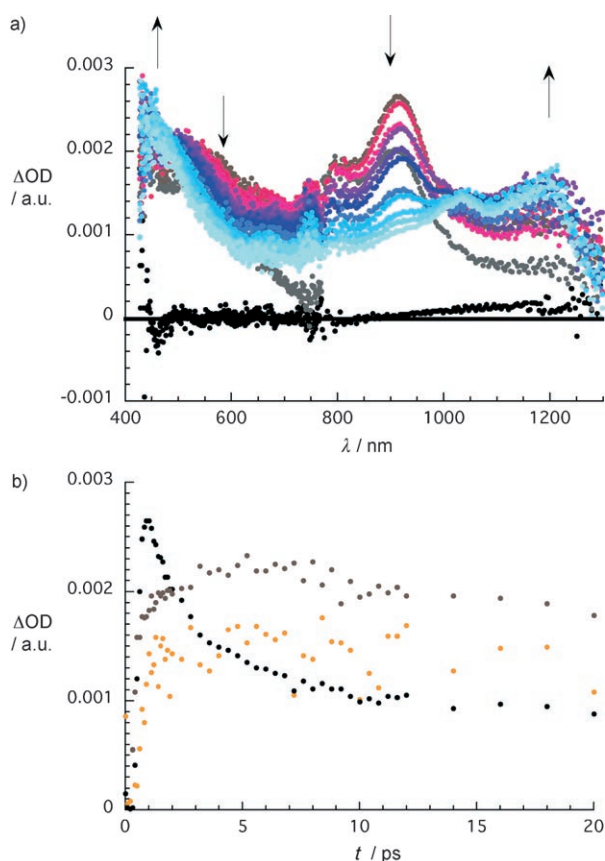
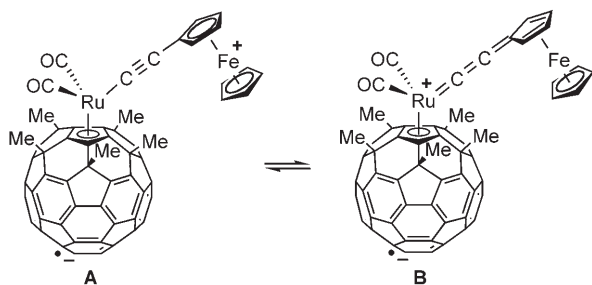


Figure 8. a) Differential absorption spectra (visible and NIR) obtained upon femtosecond flash photolysis (387 nm, 150 nJ) of **2** in nitrogen-saturated THF with several time delays between 0 and 25 ps at room temperature. The arrows indicate the temporal evolution. b) Time-absorption profiles of the spectra shown above at 470 nm (brown), 913 nm (black), and 1200 nm (orange), monitoring the charge separation.

whereas charge separation takes place only in the more polar THF. Compound **2**, on the other hand, formed the charge-separated state in both toluene and THF.

On the basis of the charge separation caused by the intramolecular electron transfer from the iron atom to the fullerene moiety of compound **2**, one can draw two resonance forms, namely, an ethynyl form **A** and an allenylidene^[22] form **B** (Scheme 2). This resonance stabilization provides a reasonable explanation for the formation of the charge-sep-



Scheme 2. The ethynyl (**A**) and allenylidene (**B**) resonance forms of compound **2**.

arated state. The feasibility of such an allenylidene ruthenium structure was previously demonstrated by the synthesis and crystal structure of the cationic allenylidene complex $[\text{Ru}(\eta^5\text{-C}_{60}\text{Me}_3)((R)\text{-prophos})(\text{C}=\text{C}=\text{CHC}_6\text{H}_4\text{NMe}_2)][\text{PF}_6]$ (prophos = 1,2-bis(diphenylphosphanyl)propane).^[22] The different effects of the acetylene and the phenylene bridges must be due to the better electrochemical communication through the former. The separations between the first and second oxidation potentials in the symmetric bisferrocene systems bearing phenylene^[23] and acetylene^[24] bridges were reported to be 131 mV ($\text{Fc-C}_6\text{H}_4\text{-Fc}$)^[23a] and 135 mV ($\text{Fc-C}\equiv\text{C-Fc}$)^[24a] respectively, and this difference is considered to show that the acetylene bridge is a better conjugative bridge than the phenylene. The structural dependency of the photo-physical properties in the present compounds illustrate how a minor structure modification of these compact molecules can change the molecular function. The availability of a variety of $\eta^5\text{-C}_{60}\text{R}_3$ ligands^[25–27] and their metal complexes^[28] provide diverse opportunities for creating organometallic molecular wires and nanoscale organic devices.^[29]

Experimental Section

General Considerations and Materials

All air- or moisture-sensitive reactions were carried out with standard Schlenk techniques. HPLC analysis was performed on a Shimadzu LC-10A system equipped with an SPD-M10A diode array detector and a Buckyprep column (Nacalai Tesque, Inc., 4.6 mm i.d. \times 250 mm). Preparative HPLC was performed on a Shimadzu LC-6AD system equipped with an SPD-6A UV detector ($\lambda = 350$ nm) and a Buckyprep column (Nacalai Tesque, Inc., 20 mm i.d. \times 250 mm). NMR spectra were recorded on a JEOL EX-400 (400 MHz) or ECA-500 (500 MHz) spectrometer. Chemical shifts are reported in parts per million with tetramethylsilane ($\delta = 0.00$ ppm) as the internal reference for ^1H and a carbonated solvent (e.g., $\delta = 77.00$ ppm for chloroform) for ^{13}C . Infrared spectra and APCI mass spectra were recorded on ReactIR 1000 and Waters ZQ2000 spectrometers, respectively. Elemental analysis was performed at the Organic Elemental Analysis Laboratory in the Department of Chemistry, The University of Tokyo. A solution of *n*BuLi in hexane was purchased from Tokyo Chemical Industry Co. Ethynylferrocene ($\text{FcC}\equiv\text{CH}$) was prepared from acetylferrocene according to the literature procedure.^[30] 4-Bromophenylferrocene ($\text{FcC}_6\text{H}_4\text{Br}$) was prepared according to the literature procedure.^[31]

Syntheses

1: Ferrocenylphenyl magnesium bromide (0.6 mL, 0.152 mmol) was added to a solution of **3** (100 mg, 0.101 mmol) in THF (20 mL) at 25 °C. The reaction mixture was stirred for 1 h at 25 °C. After removal of the solvent under reduced pressure, the mixture was diluted with toluene and filtered through a pad of silica gel. The crude product was analyzed by HPLC (toluene/2-propanol = 7:3, flow rate = 2.0 mL min⁻¹, retention time = 4.95 min). Purification with silica-gel column chromatography (toluene/hexane = 2:1) and preparative HPLC (toluene/2-propanol = 7:3; flow rate = 17 mL min⁻¹) afforded **1** (59.2 mg, 24% yield) as a red powder. ^1H NMR (CDCl_3 , 25 °C): $\delta = 2.31$ (s, 15H, C_{60}Me_3), 3.99 (s, 5H, C_5H_5), 4.26 (s, 2H, C_3H_4), 4.28 (s, 2H, C_5H_4), 7.24–7.26 (m, 2H, Ar), 7.79–7.81 ppm (m, 2H, Ar); $^{13}\text{C}\{^1\text{H}\}$ NMR ($\text{CS}_2/\text{CDCl}_3$, 25 °C): $\delta = 30.5$ (5C, C_{60}Me_3), 51.1 (5C, $\text{C}_{60}(\text{sp}^3)$), 66.3 (2C, C_3H_4), 69.1 (2C, C_5H_4), 70.0 (5C, C_5H_5), 112.8 (5C, C_{60}), 125.5 (2C, Ar), 128.2 (1C, C_3H_4), 129.2 (1C, Ar), 135.5 (1C, Ar), 143.9 (10C, C_{60}), 144.0 (10C, C_{60}), 146.2 (2C, Ar), 147.0 (5C, C_{60}), 148.2 (10C, C_{60}), 148.7 (5C, C_{60}), 152.7 (10C, C_{60}), 200.9 ppm (2C, CO); HRMS (APCI+): m/z calcd for $\text{C}_{83}\text{H}_{20}\text{FeO}_2\text{Ru}$: 1215.0560 [$M+H$]⁺; found: 1215.0586.

2: A solution of *n*BuLi (0.099 mmol) in hexane (0.062 mL) was added to a solution of ethynylferrocenyl (23.5 mg, 0.112 mmol) in THF (2.0 mL) at -78°C . The reaction mixture was allowed to warm to room temperature and was then stirred for 30 min at 25°C . The obtained reaction mixture was added to a solution of **3** (81.4 mg, 0.0823 mmol) in THF (2.0 mL) at 25°C . The reaction mixture was stirred for 10 min at 25°C . After removal of the solvent under reduced pressure, the mixture was diluted with toluene and filtered through a pad of silica gel. The crude product was analyzed by HPLC (toluene/2-propanol = 7:3, flow rate = 1.0 mL min^{-1} , retention time = 10.7 min). Purification with silica-gel column chromatography (toluene/hexane = 2:1) and preparative HPLC (toluene/2-propanol = 6:4; flow rate = 12 mL min^{-1}) afforded **2** (68.9 mg, 72% yield) as a red powder. M.p.: $220\text{--}230^{\circ}\text{C}$ (decomp.); IR (diamond probe): $\tilde{\nu}$ = 2040 (s) (C=O), 1994 (s) (C=O), 2040 cm^{-1} (s) (C≡C); $^1\text{H NMR}$ (CDCl_3 , 25°C): δ = 2.53 (s, 15H, C_{60}Me_5), 4.04 (t, J = 1.8 Hz, 2H, C_3H_4), 4.14 (s, 5H, C_5H_5), 4.28 ppm (t, J = 1.8 Hz, 2H, C_5H_4); $^{13}\text{C NMR}$ ($\text{CS}_2/\text{CDCl}_3$, 25°C): δ = 30.5 (q, $^1J_{\text{C,H}}$ = 130.8 Hz, 5C, C_{60}Me_5), 50.4 (s, 5C, $\text{C}_{60}(\text{sp}^3)$), 67.2 (d, $^1J_{\text{C,H}}$ = 176.7 Hz, 2C, 2,5- C_5H_4), 69.5 (d, $^1J_{\text{C,H}}$ = 174.4 Hz, 5C, C_5H_5), 70.4 (d, $^1J_{\text{C,H}}$ = 175.6 Hz, 2C, 3,4- C_5H_4), 106.4 (s, 1C, CCFc), 107.7 (s, 1C, 1- C_5H_4), 111.7 (s, 5C, $\text{C}_{60}(\text{Cp})$), 121.8 (s, 1C, RuCC), 143.5 (s, 10C, C_{60}), 143.5 (s, 10C, C_{60}), 146.6 (s, 5C, C_{60}), 147.8 (s, 10C, C_{60}), 148.2 (s, 5C, C_{60}), 152.0 (s, 10C, C_{60}), 196.5 ppm (s, 2C, CO); MS (APCI+): m/z = 1162 [$\text{M}]^+$; elemental analysis: calcd (%) for $\text{C}_{79}\text{H}_{24}\text{FeO}_2\text{Ru}(\text{C}_7\text{H}_8)$: C 82.36, H 2.57; found: C 81.98, H 2.94.

X-ray Crystallographic Analysis

X-ray diffraction data of **1** and **2** were collected on a Rigaku RAXIS-RAPID II imaging plate diffractometer with graphite-monochromated MoK_{α} radiation ($\lambda = 0.71075\text{ \AA}$). The structures of **1** and **2** were solved by direct methods (SIR97). The positional and thermal parameters of the non-hydrogen atoms were refined anisotropically on F^2 by the full-matrix least-squares method with SHELXL-97. The hydrogen atoms were placed at calculated positions and refined with a riding model on their corresponding carbon atoms. CCDC-666251 (**1**) and -666252 (**2**) contain the supplementary crystallographic data for this paper. These data can be obtained free of charge from The Cambridge Crystallographic Data Centre at www.ccdc.cam.ac.uk/dad_request7cif.

Electrochemical Measurements

Electrochemical measurements were performed on a BAS CV-50W voltammetric analyzer. A glassy-carbon electrode was used as the working electrode, and the counter electrode was a platinum coil. All potentials were measured against an Ag/Ag^+ reference electrode and corrected against Fc/Fc^+ . Cyclic voltammetry was performed at a scan rate of 100 mV s^{-1} . All half-wave potentials, $E_{1/2}$, are given by $(E_{\text{pc}} + E_{\text{pa}})/2$, in which E_{pc} and E_{pa} are the cathodic and anodic peak potentials, respectively.

Photophysical Studies

Femtosecond transient absorption studies were performed with 387-nm laser pulses (1 kHz, 150-fs pulse width) from an amplified Ti/sapphire laser system (Clark-MXR, Inc.). Nanosecond laser flash photolysis experiments were performed with 337-nm laser pulses from a nitrogen laser (8-ns pulse width) with front-face excitation geometry. Fluorescence lifetimes were measured with a Laser Strobe fluorescence lifetime spectrometer (Photon Technology International) with 337-nm laser pulses from a nitrogen laser fiber-coupled to a lens-based T-formal sample compartment equipped with a stroboscopic detector. Details of the Laser Strobe systems are described on the manufacturer's website. Emission spectra were recorded with an SLM 8100 spectrofluorometer. The experiments were performed at room temperature. Each spectrum represents an average of at least five individual scans, and appropriate corrections were applied when necessary.

Acknowledgements

Generous support for this collaborative research from the Alexander von Humboldt Foundation (to E.N. and S.S.G.), MEXT (KAKENHI for E.N., No. 18105004), and the Global COE Program for Chemistry Innovation is deeply acknowledged. The SFB 583, DFG (GU 517/4-1), FCI and the Office of Basic Energy Sciences of the U.S. Department of Energy are acknowledged for their financial support.

- [1] a) A. Hirsch, M. Brettreich, *Fullerenes: Chemistry and Reactions*, Wiley-VCH, Weinheim, **2004**; b) K. M. Kadish, R. S. Ruoff, *Fullerenes: Chemistry, Physics, and Technology*, Wiley-VCH, Weinheim, **2000**; c) *Fullerenes: From Synthesis to Optoelectronic Properties*, (Eds.: D. M. Guldi, N. Martin), Kluwer Academic, Dordrecht, **2002**; d) *Nuclear and Radiation Chemical Approaches to Fullerene Science*, (Ed.: T. Braun), Kluwer Academic, Dordrecht, **2000**.
- [2] C. A. Reed, R. D. Bolskar, *Chem. Rev.* **2000**, *100*, 1075–1120.
- [3] a) H. Imahori, K. Hagiwara, T. Akiyama, M. Aoki, S. Taniguchi, T. Okada, M. Shirakawa, Y. Sakata, *Chem. Phys. Lett.* **1996**, *263*, 545–550; b) D. M. Guldi, K.-D. Asmus, *J. Am. Chem. Soc.* **1997**, *119*, 5744–5745; c) S. Fukuzumi, K. Ohkubo, H. Imahori, D. M. Guldi, *Chem. Eur. J.* **2003**, *9*, 1585–1593; d) D. M. Guldi, *Spectrum* **2003**, *16*, 8–11; e) D. M. Guldi, S. Fukuzumi in *Fullerenes: From Synthesis to Optoelectronic Properties* (Eds.: D. M. Guldi, N. Martin), Kluwer, Dordrecht, **2003**, pp. 237–265.
- [4] a) H. Imahori, D. M. Guldi, K. Tamaki, Y. Yoshida, C. Luo, Y. Sakata, S. Fukuzumi, *J. Am. Chem. Soc.* **2001**, *123*, 6617–6628; b) D. M. Guldi, H. Imahori, K. Tamaki, Y. Kashiwagi, H. Yamada, Y. Sakata, S. Fukuzumi, *J. Phys. Chem. A* **2004**, *108*, 541–548; c) H. Imahori, Y. Sekiguchi, Y. Kashiwagi, T. Sato, Y. Araki, O. Ito, H. Yamada, S. Fukuzumi, *Chem. Eur. J.* **2004**, *10*, 3184–3196.
- [5] a) H. Imahori, Y. Sakata, *Adv. Mater.* **1997**, *9*, 537–546; b) M. Prato, *J. Mater. Chem.* **1997**, *7*, 1097–1109; c) N. Martin, L. Sanchez, B. Ill-escas, I. Perez, *Chem. Rev.* **1998**, *98*, 2527–2547; d) H. Imahori, Y. Sakata, *Eur. J. Org. Chem.* **1999**, 2445–2457; e) F. Diederich, M. Gomez-Lopez, *Chem. Soc. Rev.* **1999**, *28*, 263–277; f) D. M. Guldi, *Chem. Commun.* **2000**, 321–327; g) D. Gust, T. A. Moore, A. L. Moore, *J. Photochem. Photobiol. B* **2000**, *58*, 63–71; h) D. Gust, T. A. Moore, A. L. Moore, *Acc. Chem. Res.* **2001**, *34*, 40–48; i) D. M. Guldi, N. Martin, *J. Mater. Chem.* **2002**, *12*, 1978–1992; j) D. M. Guldi, *Chem. Soc. Rev.* **2002**, *31*, 22–36; k) H. Imahori, Y. Mori, Y. Matano, *J. Photochem. Photobiol. C* **2003**, *4*, 51–83; l) J. F. Nierengarten, *Top. Curr. Chem.* **2003**, *228*, 87–110; m) D. M. Guldi, *Pure Appl. Chem.* **2003**, *75*, 1069–1075; n) M. E. El-Khouly, O. Ito, P. M. Smith, F. D'Souza, *J. Photochem. Photobiol. C* **2004**, *5*, 79–104; o) D. M. Guldi, M. Prato, *Chem. Commun.* **2004**, 2517–2525; p) D. M. Guldi, *J. Phys. Chem. B* **2005**, *109*, 11432–11441; q) D. M. Guldi, F. Zerbetto, V. Geogakilas, M. Prato, *Acc. Chem. Res.* **2005**, *38*, 38–43; r) D. M. Guldi, G. M. A. Rahman, C. Ehli, V. Sgobba, *Chem. Soc. Rev.* **2006**, *35*, 471–487; s) D. M. Guldi, *Phys. Chem. Chem. Phys.* **2007**, *12*, 1400–1420; t) N. Martin, L. Sanchez, M. Heranz, B. Illescas, D. M. Guldi, *Acc. Chem. Res.* **2007**, *40*, 1015–1024.
- [6] H. Imahori, H. Norieda, H. Yamada, Y. Nishimura, I. Yamazaki, Y. Sakata, S. Fukuzumi, *J. Am. Chem. Soc.* **2001**, *123*, 100–110.
- [7] a) C. Luo, D. M. Guldi, H. Imahori, K. Tamaki, Y. Sakata, *J. Am. Chem. Soc.* **2000**, *122*, 6535–6551; b) H. Imahori, H. Yamada, D. M. Guldi, Y. Endo, A. Shimomura, S. Kundu, K. Yamada, T. Okada, Y. Sakata, S. Fukuzumi, *Angew. Chem.* **2002**, *114*, 2450–2453; *Angew. Chem. Int. Ed.* **2002**, *41*, 2344–2347.
- [8] J. Flamigni, E. Baranoff, J.-P. Collin, J.-P. Sauvage, *Chem. Eur. J.* **2006**, *12*, 6592–6606.
- [9] a) M. Sawamura, Y. Kuninobu, M. Toganoh, Y. Matsuo, M. Yamana-ka, E. Nakamura, *J. Am. Chem. Soc.* **2002**, *124*, 9354–9355; b) M. Toganoh, Y. Matsuo, E. Nakamura, *J. Am. Chem. Soc.* **2003**, *125*, 13974–13975; c) R. H. Herber, I. Nowik, Y. Matsuo, M. Toganoh, Y. Kuninobu, E. Nakamura, *Inorg. Chem.* **2005**, *44*, 5629–5635; d) Y. Matsuo, H. Isobe, T. Tanaka, Y. Murata, M. Murata, K. Komatsu, E. Nakamura, *J. Am. Chem. Soc.* **2005**, *127*, 17148–17149;

- e) Y. Matsuo, K. Tahara, E. Nakamura, *J. Am. Chem. Soc.* **2006**, *128*, 7154–7155.
- [10] D. M. Guldi, G. M. A. Rahman, R. Marczak, Y. Matsuo, M. Yamana, E. Nakamura, *J. Am. Chem. Soc.* **2006**, *128*, 9420–9427.
- [11] a) M. Maggini, G. Scorrano, M. Prato, *J. Am. Chem. Soc.* **1993**, *115*, 9798–9799; b) M. Prato, M. Maggini, *Acc. Chem. Res.* **1998**, *31*, 519–526.
- [12] Y. Matsuo, E. Nakamura, *Organometallics* **2003**, *22*, 2554–2563.
- [13] a) M. Sawamura, H. Iikura, E. Nakamura, *J. Am. Chem. Soc.* **1996**, *118*, 12850–12851; b) Y. Matsuo, A. Muramatsu, K. Tahara, M. Koide, E. Nakamura, *Org. Synth.* **2006**, *83*, 80–87.
- [14] M. Sato, H. Shintate, Y. Kawata, M. Sekino, M. Katada, S. Kawata, *Organometallics* **1994**, *13*, 1956–1962.
- [15] a) H. Iikura, S. Mori, M. Sawamura, E. Nakamura, *J. Org. Chem.* **1997**, *62*, 7912–7913; b) M. Sawamura, Y. Kuninobu, E. Nakamura, *J. Am. Chem. Soc.* **2000**, *122*, 12407–12408; c) Y. Kuninobu, Y. Matsuo, M. Toganoh, M. Sawamura, E. Nakamura, *Organometallics* **2004**, *23*, 3259–3266; d) Y. Matsuo, A. Iwashita, E. Nakamura, *Organometallics* **2005**, *24*, 89–95.
- [16] M. Sawamura, M. Toganoh, Y. Kuninobu, S. Kato, E. Nakamura, *Chem. Lett.* **2000**, 270–271.
- [17] Data not shown; for details, see reference [9].
- [18] Y. Matsuo, Y. Kuninobu, S. Ito, E. Nakamura, *Chem. Lett.* **2004**, *33*, 68–69.
- [19] This maximum was not seen in our recent pulse radiolysis investigation because it lies outside the spectroscopic limits of the detector.
- [20] Y. Matsuo, E. Nakamura, *J. Am. Chem. Soc.* **2005**, *127*, 8457–8466.
- [21] The charge separation with a lifetime of 5.5 ps in toluene is notably faster than the accelerated intersystem crossing seen in **1** (21 ps).
- [22] Y.-W. Zhong, Y. Matsuo, E. Nakamura, *Chem. Asian J.* **2007**, *2*, 358–366.
- [23] a) E. E. Bunel, P. Campos, J. Ruz, L. Valle, I. Chadwick, M. S. Ana, G. Gonzalez, J. M. Manriquez, *Organometallics* **1988**, *7*, 474–476; b) R. Chukwu, A. D. Hunter, B. D. Santarsiero, S. G. Bott, J. L. Atwood, J. Chassagnac, *Organometallics* **1992**, *11*, 589–597; c) C. Patoux, C. Coudret, J.-P. Launay, C. Joachim, A. Gourdon, *Inorg. Chem.* **1997**, *36*, 5037–5049.
- [24] a) C. LeVanda, D. O. Cowan, C. Leitch, K. Bechgaard, *J. Am. Chem. Soc.* **1974**, *96*, 6788–6789; b) R. D. Adams, B. Qu, M. D. Smith, *Organometallics* **2002**, *21*, 3867–3872.
- [25] a) E. Nakamura, K. Tahara, Y. Matsuo, M. Sawamura, *J. Am. Chem. Soc.* **2003**, *125*, 2834–2835; b) Y. Matsuo, K. Tahara, M. Sawamura, E. Nakamura, *J. Am. Chem. Soc.* **2004**, *126*, 8725–8734; c) Y. Matsuo, K. Tahara, K. Morita, K. Matsuo, E. Nakamura, *Angew. Chem.* **2007**, *119*, 2902–2905; *Angew. Chem. Int. Ed.* **2007**, *46*, 2844–2847.
- [26] a) M. Sawamura, K. Kawai, Y. Matsuo, K. Kanie, T. Kato, E. Nakamura, *Nature* **2002**, *419*, 702–705; b) Y. Matsuo, A. Muramatsu, R. Hamasaki, N. Mizoshita, T. Kato, E. Nakamura, *J. Am. Chem. Soc.* **2004**, *126*, 432–433; c) Y. Matsuo, A. Muramatsu, Y. Kamikawa, T. Kato, E. Nakamura, *J. Am. Chem. Soc.* **2006**, *128*, 9586–9586; d) Y.-W. Zhong, Y. Matsuo, E. Nakamura, *J. Am. Chem. Soc.* **2007**, *129*, 3052–3053.
- [27] a) Y.-W. Zhong, Y. Matsuo, E. Nakamura, *Org. Lett.* **2006**, *8*, 1463–1466; b) A. Iwashita, Y. Matsuo, E. Nakamura, *Angew. Chem.* **2007**, *119*, 3583–3586; *Angew. Chem. Int. Ed.* **2007**, *46*, 3513–3516.
- [28] a) M. Toganoh, Y. Matsuo, E. Nakamura, *Angew. Chem.* **2003**, *115*, 3654–3656; *Angew. Chem. Int. Ed.* **2003**, *42*, 3530–3532; b) Y. Matsuo, E. Nakamura, *Inorg. Chim. Acta* **2006**, *359*, 1979–1982; c) Y. Matsuo, Y. Mitani, Y.-W. Zhong, E. Nakamura, *Organometallics* **2006**, *25*, 2826–2832.
- [29] F. Paul, C. Lapinte, *Coord. Chem. Rev.* **1998**, *431*, 178–180.
- [30] M. Rosenblum, N. Brown, J. Papenmeier, M. Applebaum, *J. Organomet. Chem.* **1966**, *6*, 173–180.
- [31] V. M. Makarov, P. V. Dyadchenko, M. Y. Antipin, *Russ. Chem. Bull.* **2004**, *53*, 2768–2773.

Received: November 15, 2007
Published online: April 9, 2008